IISc Theses Abstracts

Contents

J. Indian Inst. Sci., Mar.–Apr. 1996, **76**, 291–322.

IISc THESES ABSTRACTS

Thesis Abstract (Ph. D.)

Behaviour of the germ-cell specific lamin through mammalian spermatogenesis as probed with monoclonal antibodies by K. Manjula

Research supervisors: M. R. S. Rao and Anjali A. Karande
Department: Biochemistry

1. Introduction

One of the definitive features of eucaryotic cells is the existence of a membranous nuclear envelop that creates a distinct compartmentalisation between the nucleus and the cytoplasm. The nuclear envelop comprises the outer and the inner nuclear membranes, the nuclear pore complexes and the nuclear lamina. In higher eucaryotes, the nuclear envelops disassemble into vesicles and soluble components during mitosis. These components later reassemble in an ordered fashion to form the daughter nuclei. The nuclear lamina is a purely proteinaceous structure and contains very few (1–3) major polypeptides with molecular weights ranging from 60 to 80 kDa. Dynamic changes occur in the nuclear lamina during the process of mitosis.

While several laboratories have focused attention on the fate of the nuclear lamina during mitosis, very little information is known on the fate of the nuclear lamina during meiosis.

From a genetic point of view, the main purpose of sexual reproduction is to provide successive generations with new combinations of linked and unlinked genes. This is achieved by two alternating processes *viz.*, meiosis and fertilisation.

For the past several years, our laboratory has been interested in studying the process of meiosis and the events associated with this process, using the rat testes as the model system. In this regard, our laboratory had earlier identified a 120 kDa polypeptide unique to the germ cells of the rat testes[1] in various stages of spermatogenesis. This was later shown to be a homodimer of a 60 kDa germ-cell specific lamin that exhibited dynamic changes in its localisation during the process of meiosis. Using polyclonal antisera raised against this unique protein, it was shown to be related, but not identical to somatic lamin B. This finding was later reinforced by a comparative peptide mapping of the two polypeptides.

Our interest was to generate specific monoclonal antibodies against this lamin polypeptide. Therefore, the work was initiated with the following objectives in mind:

a) To obtain monoclonal antibodies to this unique ln g.

b) To study the cross-reactivity of these MAbs with somatic lamins, and

c) To study the fate of the germ-cell specific lamin during meiosis by immunolocalisation studies using these MAbs.

2. Experimental

The first step was to obtain the polypeptide in a pure form in order to establish a hybridoma. To this end, the 60 kDa lamin was cut out from several SDS polyacrylamide gels of the lamina fraction, from sonication-resistant spermatid nuclei, isolated from the rat testes. Several such bands

were also used to immunise mice. A new method of sub-dermal placement of a polypeptide was used to immunise mice against microgram quantities of this protein.

This protein was later purified using the process of electroelution of the bands cut out from several polyacrylamide gels, stained with 0.5 M KCl.

Once the hybridoma was established using a standard protocol[2] two levels of screening were followed for selecting the lamin g antibody-secreting clones. The first level of screening was that of the parent clones. Dot-binding assay, ELISA, SPRIA and immunoblotting were the various screening methods used at this level. Positive parent clones were then subjected to sub-cloning by limiting dilution. The clones obtained at this stage were rescreened by conducting an ELISA for mouse IgG secretors, and finally by immunoblotting. In this manner, eight monoclonal antibodies to the germ-cell-specific lamin were selected. The clones were duly named as $A_{11}C_7$, $A_{11}D_4$, C_1F_7, C_1G_8, C_8B_3, C_8C_5, A_2C_2 and D_9E_6. Isotyping of these monoclonal antibodies revealed that they all belonged to the subtypes of the IgG class.

Cross-reactivity of these MAbs with somatic liver lamins was checked both by immunoblotting as well as immunofluorescence. Using both these methods it was revealed that only two of the eight monoclonal antibodies exhibited a faint cross-reactivity against the somatic liver lamin B ($A_{11}C_7$ and $A_{11}D_4$). An immunofluorescence study revealed that the pattern of staining of liver nuclei differed between the two MAbs. This suggests that they may be recognising two different epitopes of the somatic lamin B and the germ-cell-specific lamin.

Immunolocalisation studies were carried out using various cell types in germ cells in the rat testes. Based on these observations, the MAbs could be classified into the following categories:

a) Those exhibiting a strong fluorescence

b) Those exhibiting a weak fluorescence

c) Those exhibiting no fluorescence.

The pattern of localisation was as follows in the various cell types:

1) Pre-meiotic spermatogonia—laminar

2) Pachytene spermatocytes—phase-dense regions

3) Post-meiotic round spermatids—laminar.

Double-antibody staining of pre-meiotic spermatogonial nuclei was carried out to gain an insight into the co-existence of the germ cell-specific lamin and the somatic liver lamin B. It was found that, in accordance with the model proposed earlier by Sudhakar and Rao[3], both these lamins co-existed in the pre-meiotic nuclei. It was interesting to note that while the somatic lamins were undetected in the germ cells that were either undergoing meiosis or had already undergone meiosis, they seemed to co-exist in the pre-meiotic germ cells with no obvious role to play. What happens to this lamin during the later stages of spermatogenesis is an interesting question in itself which can be looked into in the future.

Another interesting question we wanted to address in our study is the fate of the germ cell-specific lamin during the pachytene stage of meiotic prophase I. As noted earlier in the immunofluorescence study, the pattern of localisation of ln g in this stage was diffused and distributed in the nucleus. We therefore wanted to take a closer look into this phenomenon by treating pachytene nuclei with a hypotonic salt solution, and thereafter observe their localisation in such surface spread nuclei. In this manner, by immunostaining surface-spread pachytene spermatocytes the antigen was further localised at the telomeric ends of the paired homologous chromosomes. We therefore speculate that this protein has a role in facilitating the attachment of these chromo-

somes to the inner nuclear membrane. By a prolonged treatment of the nuclei to the hypotonic salt solution, it was further noticed that even though the nuclear membrane was totally disrupted, the antigen was still localised at the ends of the paired homologous chromosomes.

All of the immunolocalisation studies conducted so far were on isolated nuclei fixed on to glass slides. We therefore wanted to look into the localisation of this polypeptide in thin sections of a seminiferous tubule. An *in-situ* immunostaining of thin sections of seminiferous tubules of the rat was carried out. Both paraffin-embedded as well as cryosections were used. The methods of staining followed were both the FITC method as well as the HRP method. Staining the tubules with either of these methods revealed that in both the pachytene spermatocytes as well as in round spermatids the antigen was localised at the nuclear rim, thereby ascertaining that the fluorescence seen in isolated nuclei was not an artefact of the isolation protocol followed.

3. Conclusion

To summarise, we have obtained eight monoclonal antibodies to the germ cell-specific lamin. Using these monoclonal antibodies, we have been able to obtain a clearer picture of the localisation of the polypeptide in the various cells of the rat testes. We have also been able to observe the extent of cross-reactivity of the germ cell-specific lamin and its counterpart, the somatic liver lamin B. Immunohistochemical staining of the seminiferous tubules of the rat testes revealed that the pattern of staining observed *in situ* matched the pattern observed in the isolated nuclei.

A closer look into the pattern of staining in pachytene nuclei by the surface spreading of the nuclei revealed an interesting finding. It looks as if the antigen was involved in anchoring the paired homologous chromosomes to the inner nuclear membrane *via* the telomeric ends of these chromosomes. Further work, however, has to be carried out in order to reinforce this statement.

References

1. BEHAL, A., KULKARNI, P. AND RAO, M. R. S. — *J. Biol. Chem.*, 1987, **262**, 10898–10902.
2. WESTERWOUDT, R. J., NAIPAL, A. M. AND HARRISON, C. M. H. — *J Immun Meth.*, 1984, **68**, 89–101.
3. SUDHAKAR, L. AND RAO, M. R. S. — *J Biol Chem*, 1990, **265**, 22526–22532.

Thesis Abstract (Ph. D.)

Phytohormone regulated *α*-amylase expression during somatic embryogenesis in sandalwood (*Santalum album* L.) by Mridula L. Subramanyam

Research supervisors: G. Lakshmi Sita and K. P. Gopinathan

Department: Microbiology and Cell Biology

1. Introduction

Sandalwood (*Santalum album* L.) is a forest tree of immense economic importance. *In-vitro* approaches have potential in tree improvement. They help in the clonal propagation of this depleting species which has been otherwise difficult to propagate by conventional methods on account of sexual incompatibility and low seed viability[1]. Currently this system has been exploited to study differential gene expression during embryogenesis. In general, very little information is

available on gene expression in forest trees. Somatic embryos of sandalwood therefore serve as an ideal model system to study the regulation of gene expression. Hormonal balance plays a critical role during the differentiation of somatic embryos[2]. Much effort has been directed to study the effect of gibberellic acid at the molecular level taking *a*-amylase as a marker. Among the several hydrolases induced by GA, *a*-amylase is induced maximally[3]. The *a*-amylases constitute a multi-gene isoenzyme family and are divided into two major groups depending on their pI values, *viz*, high and low pI values[4–6]. The two groups respond differentially[7] to the addition of GA, ABA and Ca^{2+}. We report here the induction of *a*-amylase by GA during somatic embryogenesis in sandal-

atagctaaattgctggatcccaatccccagttcgaggatgaccatcgaaaccctgagtaa
L N C W I P I P S S R M T I E T L S N

cacaactgggtgcaaaaaggcccgccacaaagttggacctcaataccaagggcatcgtca
T T G C K K A R H K V G P Q Y Q G H R Q

atgtcgacctcgcgtgctcgaattcgcagcggcgccacattgactgcaagtcgccgggca
C R P R V L E F A A A P H * L Q V A G H

tgatagcgtcgtggcttttccttcggcggggaccaataccgcggagggaagaagtatatg
D S V V A F P S A G T N T A E G R S I C

tggcccggcgcttcggacagggtcgcgcagagggtatgagagcatccggaagaaccaagg
G P A L R T G S R R G Y E S I R K N Q G

gtacccatgcatcgtgagggaaatcggggcaatagaggatatcaaaaaattttgttcttt
Y P C I V R E I G A I E D I K K F C S F

ttggtgtttgccggaaaataattgtgaaggttgtgcccgtcgatcacgtcttcgagtgtg
W C L P E N N C E G C A R R S R L R V *

aagtgaaagaggagcgagatcgattcggatctttggggattcggtagggagtgaatcccc
S E R G A R S I R I F G D S V G S E S P

agagcaagatgcagggcctggtgacagttgccttcattggccaataaactggatgggcat
E Q D A G P G D S C L H W P I N W M G I

caagatgattgggactaaaaacaatgtcggaaaatttttccttgcttcaacgtgttcg
K M I G T K N N V G K F F P L L Q R V R

aggtttgtgatgacttctaatgtatgttcgcacgtgtatcgctggtttgacggagggtctc
G L * * L * C M F A R V S L V * R R V S

tacattgttgtccaagctttgtttgcccttatatttttaaaattaatatttcctcgtgtt
T L L S K L C L P L Y F * N * Y F L V F

taaggggagcattttggacatccataaatttttttaaaataaatcctttgaatttta
K G S I L D I H K F F L N K S F E F

FIG. 1. The nucleotide and predicted amino acid sequence of sandalwood α-amylase. The nucleotide sequence of the cDNA insert in clone *pSamR* was 777 bp long and cover the 3' end of the α-amylase gene. The restriction enzyme sites identified have been underlined

wood. The response to GA and antagonist ABA has also been investigated. We also report the isolation of *a*-amylase partial cDNA clone using the induced mRNA.

2. Results and discussion

The somatic embryos were induced from the callus initiated using the stem pieces from 20–25-year old sandalwood trees as the explant. Somatic embryos were best obtained on an MS medium supplemented with GA. A progressive increase in the *a*-amylase activity was seen throughout the development of somatic embryos. There was a 40-fold induction of the enzyme activity in the somatic embryos over that of the callus or undifferentiated tissue. Isoenzymes of *a*-amylase were characterised—callus showed two enzymatically active bands corresponding to low pI values 5.3 and 5.4 while the somatic embryos showed high pI isoenzyme bands of 6.8 and 6.35. The apparent molecular weight of the enzyme in the somatic embryos was estimated from SDS-PAGE and by Western blot analysis to be 45 kDa and stained positive for glycosylation. Comparative studies with *a*-amylase from zygotic embryos revealed it to be a distinct species differing in molecular weight. The inducibility of *a*-amylase by GA was confirmed by using two inhibitors, sodium butyrate and ABA. Sodium butyrate inhibits GA-induced *a*-amylase[8]. In the case of somatic embryos there was virtually complete inhibition, at 5 mM treated for 24 hours, which was reversible. ABA, another growth regulator, is an antagonist to GA[9]. The effect of ABA on somatic embryos is unique. At lower concentrations there was characteristic inhibition of *a*-amylase activity in the somatic embryos. But at higher concentrations there was derepression of the activity. This is a novel observation not reported before in any other system. A similar profile was seen at the RNA level. Further analysis using native-PAGE and IEF-PAGE showed that the increase in specific activity at higher ABA concentrations due to derepression resulted in *de-novo* synthesis of a new isoenzyme. In the case of barley aleurone system it has been reported that there is inhibition in a concentration-dependent manner[10–13]. The observed response using a known antagonist ABA which in this case derepresses enzyme activity strongly suggests a marked difference in the regulation of the gene during differentiation in somatic embryos. Two possibilities could exist that may be responsible for the unique response of somatic embryos to ABA: (a) Somatic embryos exist in a different environmental condition as compared to the zygotic embryos. There is neither the aleurone layer nor the endosperm which is the site for *a*-amylase synthesis. (b) There could be an increase in the endogenous gibberellin levels at higher ABA concentrations[14] which could be responsible for the increase in the activity of *a*-amylase. As a preliminary step to facilitate the study of *a*-amylase gene regulation and expression at the molecular level a partial *a*-amylase c-DNA clone has been isolated. A c-DNA library was constructed from the mRNA from somatic embryos. The library was probed with *a*-amylase gene from barley. The 800-bp clone, termed *pSamR* has been characterised with respect to its restriction enzyme sites and putative glycosylation sites. The nucleotide sequence of the clone has been determined. With the availability of the partial cDNA clone it would be possible to look further into the regulation of enzyme induction during differentiation. This could then be further extended to elucidate the mechanism of hormone action during differentiation in somatic embryos (Fig. 1).

References

1. LAKSHMI SITA, G. — In *Cell and tissue culture*, Vol. 2 (Bonga, J. M. and Durzan, D. J., eds), 1987, pp. 363–374, Martinus Nijhoff.
2. TULECKE, W. — In *Cell and tissue culture*, Vol. 2 (Bonga, J. M. and Durzan, D. J., eds), 1987, pp. 61–91, Martinus Nijhoff.
3. CHANDLER, P. M. *et al.* — *Pl. Mol. Biol.*, 1984, **3**, 407–418.

4.	ROGERS, J C.	*J. Biol Chem.*, 1985, **260**, 3731–3738.
5.	CALLIS, J. AND HO, T D. H.	*Arch. Biochem. Biophys.*, 1983, 224–234
6.	KHURSHEED, B. AND ROGERS, J. C.	*J Biol Chem.*, 1988, **263**, 18953–18960.
7.	FINCHER, G B.	*A Rev. Pl. Physiol. Pl Mol. Biol*, 1989, 305–346.
8.	KUMAR, S. *et al.*	*Pl. Mol. Biol*, 1985, **5**, 269–279
9.	NOLAND, R. C. AND HO, T. D. H	*Planta*, 1988, **174**, 551–560.
10.	KNOX, C. A. P. *et al.*	*Pl Mol. Biol.*, 1987, **9**, 3–17.
11.	BAULCOMBE, D. C. *et al.*	*Mol. Gen. Genet.*, 1987, **209**, 33–40.
12.	HIGGINS, T. J. V. *et al*	*Nature*, 1976, **260**, 166–169.
13.	NOLAN, R. C. *et al.*	*Pl Mol. Biol.*, 1987, **8**, 13–22.
14.	RAILTON, I. D. AND WAREING, P. F.	*Planta*, 1973, **12**, 65–69.

Thesis Abstract (Ph. D.)

A search for additional genes affecting sex determination in *Drosophila melanogaster* by Anuranjan Anand

Research supervisor: H. Sharat Chandra
Department: Microbiology and Cell Biology

1. Introduction

In *Drosophila melanogaster*, the primary signal for sex determination is the ratio of the number of X chromosomes to the number of sets of autosomes[1]. This parameter, the X:A ratio, is measured very early in development and the signal is conveyed to an X-linked master 'switch' gene *sex-lethal* (*Sxl*)[2]. An X:A ratio of 1 results in the transcriptional activation of *Sxl* and this is essential for female development. Once *Sxl* has been activated in this manner, the primary signal is not necessary for maintenance of *Sxl* activity during subsequent development because the sex-specific activity of the gene is autoregulated[3]. Activation of *Sxl* leads to appropriate regulation by RNA splicing of downstream genes concerned with somatic sex determination[4]. When the X:A ratio equals 1/2, *Sxl* is ineffective and male development ensues. Germline sex determination and dosage compensation are also under the control of *Sxl*[5,6]. An outline of sex determination and dosage compensation pathways and the genes participating in them is schematically shown in Fig. 1.

2. Results and discussion

In the present study an attempt was made to identify, by deficiency analysis, regions of the X chromosome that may contain additional genes affecting sex determination. A screen was set up in which deficiencies uncovering different regions of the X chromosome were made heterozygous with Sxl^{fl}, a null allele. It was reasoned that, if the deficiency uncovers gene(s) which may perform a role in the sex determination pathway, then it may lower the probability of appropriate regulation of *Sxl* because in Sxl^{fl}/Sxl^{+} heterozygotes the product levels of *Sxl* may have already been reduced to barely sufficient levels. Seven out of the 25 deficiences tested in this manner showed interaction in the sense that significant levels of female lethality were observed. Four of these deficiencies uncover regions which were not hitherto known to contain sex determination

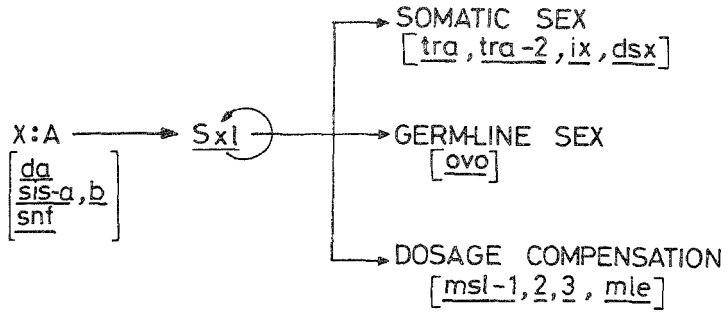

FIG 1.

genes. These newly identified regions are defined by deletions RA2 (7D10;8A4-5), KA14(7F1-2;8C6), C52(8E;9C,D) and N19(17A1-18A2).

In a parallel approach, an EMS mutagenesis experiment was set up to recover X-linked lesions affecting female viability. Two female-specific lethals (Sxl^{dlf} and *flex*) and five mutations showing synergistic female lethality (*fl*-35, *fl*-43, *fl*-46, 231 and 570) in combination with Sxl^{fl} were recovered. Approximate map positions of five of these mutations were determined on the basis of recombination data. One of them (Sxl^{dlf}) maps to the same genetic interval in which *Sxl* is located. Map positions of *flex* and *fl*-43 are, 1-54 and 1-30, respectively. *fl*-35 is located at least 4.6 cM and *fl*-46 at least 4.9 cM away from *sn* (1–21.0), towards the centromere. None of these mutations except Sxl^{dlf} seems to be allelic to known sex determination genes. Genetic characterisation of these five mutations was attempted and the results were as follows.

As noted above Sxl^{dlf}, a female-specific lethal mutation, is an allele of *Sxl*. Sxl^{dlf} did not complement Sxl^{fLS}, $Sxl^{fm7,M1}$ and $Sxl^{M1,fm3}$, three late function-defective mutations in this gene, but it complemented Sxl^{f9}, an early function-defective mutation. This suggests that Sxl^{dlf} is defective in the late functions of *Sxl*.

flex is a female-specific lethal mutation on the *X*. *flex* does not show female lethality in *trans*heterozygous combination with mutations in any of the following genes: *Sxl*, *sis-a*, *sis-b*, *da* and *fl*(2)*d*. *flex* could not be rescued by providing Sxl^{+} in the form of a duplication or by a *hs-Sxl* transgene.

Three mutations, *fl*-43, *fl*-35 and *fl*-46, show synergistic female lethality in combination with Sxl^{fl}. None of these mutations show significant interactions with *sis-a*, *sis-b* or *da*, three genes needed for transcriptional activation of *Sxl*. Female lethality due to interactions between Sxl^{fl} and Sxl^{dlf}, *fl*-35, *fl*-43 and *fl*-46 could be rescued by providing Sxl^{+} in the form of a duplication, indicating that lethality could be due to a reduction in *Sxl* product levels in the double mutant combinations.

Regulation of *Sxl* occurs in two steps. The first of these involves its transcriptional activation early during embryogenesis in response to the X:A ratio elements (*sis-a*, *sis-b* and *runt*). The second step involves maintenance of this active status by an autoregulatory loop which includes

differential RNA splicing[7]. *sis-a, sis-b* and *runt* show dose-dependent, reciprocal, sex-specific interactions amongst themselves and with the target gene Sxl^{8-11}). These genes are functionally related because a defect in one of them can be partly offset by a duplication of one of the remaining two genes. Although the interactions among genes forming the X:A signal are reasonably well understood, we do not know the nature of interactions among genes needed for processing the *Sxl* transcripts. In fact, only two genes affecting these functions are known: *snf* and *fl(2)d*. *snf* shows interaction with Sxl^{f1}, whereas *fl(2)d* does not. As mentioned earlier, *flex, fl*-35, *fl*-43 and *fl*-46 did not show significant interaction with *da, sis-a* and *sis-b*, suggesting that none of these four genes is likely to be a part of the X:A signal. However, the interaction of these mutations with Sxl^{f1} indicates that they may be involved in the processing of *Sxl* transcripts.

References

1. BRIDGES, C. B. *Science*, 1921, **54**, 252–254.
2. CLINE, T. W. *Genetics*, 1978, **90**, 683–698.
3. CLINE, T. W. *Genetics*, 1984, **107**, 231–277.
4. BAKER, B. S. *Nature*, 1989, **340**, 521–524.
5. PAULI, D. AND MAHOWALD, A. P. *Trends Genet.*, 1990, **6**, 259–264.
6. LUCCHESI, J. C. AND MANNING, J. E. *Adv. Genet*, 1987, **24**, 371–429.
7. BELL, L. R. *et al.* *Cell*, 1991, **65**, 229–239.
8. CLINE, T. W. *Genetics*, 1988, **119**, 829–862.
9. TORRES, M. AND SÁNCHEZ, L. *EMBO J.*, 1989, **8**, 3079–3086.
10. TORRES, M. AND SÁNCHEZ, L. *Genet. Res.*, 1992, **59**, 189–198.
11. DUFFY, J. B. AND GERGEN, J. P. *Genes Dev.*, 1991, **5**, 2176–2187.

Thesis Abstract (Ph. D.)

***In vitro* and *in vivo* effects of nucleic acid reactive antibodies on transformed cells** by Chandira Kala Kumar

Research supervisors: A. Antony and G. Ramananda Rao
Department: Microbiology and Cell Biology

1. Introduction

Nucleic acid reactive antibodies have been extensively used in various biochemical investigations[1]. Inhibition of growth of transformed cells using cytotoxic agents coupled with macromolecular carriers can be achieved by exploiting the higher endocytic activity of these cells as compared to normal cells[2]. Similarly, macromolecules such as nucleic acid reactive antibodies, which are capable of inhibiting vital cellular functions[3], may also be used to achieve selective inhibition of the growth of transformed cells. The present study was undertaken to investigate: (i) The effect of antibodies on guanosine, GMP, and tRNA on normal and transformed cells grown *in vitro*, (ii) Pinocytosis in cells grown *in vitro* using gelonin as a marker, (iii) The potential of these antibodies to inhibit various nucleic acid functions in cell-free systems, and (iv) Effect of these antibodies on tumour-bearing mice.

2. Experimental

Guanosine and GMP were coupled to BSA by periodate[4] and carbodiimide methods,[5] respectively. tRNA was electrostatically complexed with methylated BSA. Antibodies to these conjugates were raised in rabbits and IgG was obtained by sodium sulphate fractionation method[6]. Binding of these antibodies to their respective haptens and various nucleic acids was studied using avidin–biotin microELISA[7] and gel retardation assay.

3. Results and discussion

Antibodies to guanosine, GMP and tRNA were raised in rabbits and characterised by avidin–biotin micro ELISA and gel retardation assay. Guanosine antibodies were found to be base specific and bind to native DNA, denatured DNA, tRNA, rRNA, poly $(A)^+$ RNA and ribosomes. The binding to DNA was also shown using pBR322 and pSVSal DNA in gel retardation assay. Antibodies raised against GMP and tRNA were shown to bind more with RNA and little with DNA.

These antibodies inhibited both the growth as well as cell number of transformed cells such as HeLa, HFS9, HEp2 and SP2/0 as monitored by the incorporation of radioactive precursors into DNA, RNA and protein. The effect was specific since they did not inhibit the growth of mouse splenocytes and calf kidney cells used as controls. The fact that immunised animals remained healthy, supported the view that the normal cells are not affected. Normal rabbit IgG and BSA antibodies failed to inhibit macromolecular synthesis in any of the cells used. HeLa and SP2/0 cells treated with GMP antibodies were shown to grow at a reduced rate and had high mean generation time as compared to control cells. Gelonin, a ribosome-inactivating protein, was used as a marker to study pinocytosis. Its only mode of entry into the cells is by pinocytosis, because it does not have receptors on the cell membrane. Inhibition of protein synthesis in the presence of gelonin as monitored by the incorporation of a radioactive precursor was observed in transformed cells but not in normal cells grown *in vitro*. This indicated a high rate of pinocytosis in transformed cells.

In order to understand the mechanism of inhibition by these antibodies, their effect on various nucleic acid-mediated functions in cell-free systems was studied. Antibodies to guanosine, GMP and tRNA inhibited *in vitro* aminoacylation of tRNA and translation of endogenous mRNAs in rabbit reticulocytes in a dose-dependent and hapten-specific manner. Guanosine antibodies inhibited *in vitro* transcription using *E.coli* RNA polymerase and calf thymus DNA in a dose-dependent manner. The inhibition was specific as it could be reversed by homologous hapten. Antibodies to GMP and tRNA did not show inhibition of *in vitro* transcription and DNA synthesis. Guanosine antibodies showed 25% inhibition of *in vitro* DNA synthesis using *E coli* DNA polymerase I.

Pre-immunisation of mice with BSA-guanosine, BSA-GMP and methylated BSA–tRNA conjugates increased the life span of mice bearing Dalton's lymphoma ascites tumour. Injection of gelonin intraperitoneally to mice bearing Dalton's tumour (used as a positive control) increased the life span of the mice. However, pre-immunisation with nonspecific proteins did not show any effect on mice bearing Dalton's tumour.

The potential of RNA reactive antibodies to inhibit nucleic acid functions *in vitro* and *in vivo* coupled with high endocytic activity of transformed cells as compared to normal cells, may offer a promising approach to selectively inhibit the growth of transformed cells.

References

1. STOLLAR, B. D. — *CRC Crit. Rev. Biochem.*, 1986, **20**, 1–36.
2. ARNOLD, L. J. JR — *Methods in Enzymology* (Widder, K. J. and Gran, R., eds) 1985, Vol. 112, pp. 270–285, Academic Press
3. MAKAROVA, O. V. AND GOLDFARB, G. M. — *Immun. Lett.*, 1979, **1**, 43–48.
4. ERLANGER, B. F. AND BEISER, S. M. — *Proc. Natn. Acad. Sci. USA*, 1964, **52**, 68–74.
5. HUMAYUN, M. AND JACOB, T. M. — *Biochim. Biophys. Acta*, 1973, **331**, 41–53.
6. HEIDE, K. AND SCHWICK, H. G. — *Handbook of experimental immunology* (Wein, D. M., ed.), 1978, p. 7.1, Blackwell Scientific Publications.
7. VAISHNAV, Y. N. AND ANTONY, A. — *Biochem. Biophys. Res. Commun.*, 1988, **154**, 118–123.

Thesis Abstract (Ph. D.)

Isolation and characterisation of poly(A)$^+$ messenger ribonucleo-protein complexes from *Candida utilis* by Sucheta G. Pai

Research supervisors: G. Ramananda Rao and M. S. Shaila

Department: Microbiology and Cell Biology

1. Introduction

Eukaryotic cytoplasmic mRNA exists as a nucleoprotein and is referred to as messenger ribonucleoprotein complex (mRNP) or informosome. The cytoplasmic mRNP complexes have two distinct locations. The mRNPs that form an integral component of the polysomal complex being translated are referred to as polysome-associated mRNPs (PmRNPs). The mRNPs that are not associated with the polysomes and are thus free in the cytoplasm are called free messenger ribonucleoprotein complexes (FmRNPs). The FmRNPs include mRNAs in transit from the nucleus to the cytoplasmic site of protein synthesis or nontranslated excess mRNAs or stored (masked) mRNAs which are to be translated later under specific physiological conditions.

Review of the literature indicates that there is not much information available on mRNP complexes and their role in regulating mRNA translatability in yeasts. Yeast, though a seemingly simple unicellular organism, has all the organisational complexities of a higher eukaryote. Therefore, the present study is aimed at isolating and characterising poly(A)$^+$ messenger ribonucleoproteins from *C. utilis*. This study on the regulation of translatibility of mRNA by informosomal proteins in *C. utilis* should provide vital clues regarding regulation at the translation level by mRNPs in higher eukaryotes.

2. Materials and methods

Candida utilis CBS 4511 obtained from the Centraalbureau voor Schimmelcultures, Delft, The Netherlands, was used in the studies. The organism was maintained by subculturing once in 15 days on Sabouraud's glucose agar plants. The basal medium for the cultivation of *C. utilis* was prepared essentially according to the formula of Wickerham[1].

The PmRNP and FmRNP complexes were isolated from the polysomal and post-polysomal fractions of *C. utilis* by thermal oligo(dT)-cellulose chromatography[2]. The pure polysomes were dissociated and fractionated to obtain PmRNA and PmRNP complexes. The post-polysomal pellet was used as a source of FmRNA and FmRNP. The fractions eluted from the column at 4°C in both instances represent naked mRNA whereas the 45°C fractions represent mRNP complexes. A high salt buffer was used to wash the column to eliminate the nonspecific protein interactions with the column.

3. Results and discussion

3.1. *Nucleoprotein nature of the isolated mRNPs*

To prove that the 45°C eluted fractions represent nucleoprotein complexes, the following criteria were used: their $A_{260\,nm}/A_{280\,nm}$ absorbancies (1.19–1.37), their buoyant densities on CsCl density gradient centrifugation[3] (1.38 g/cc for PmRNPs; 1.35 g/cc for FmRNPs) and by nitrocellulose binding assay[4].

The ultrastructural studies of mRNPs showed that these comprise linear RNA molecules with proteins attached all along. These structures were no longer seen on preincubating the samples with ribonucleases. Both PmRNP and FmRNP complexes were found to be translatable in the rabbit reticulocyte lysate *in vitro* translation system[5]. Their mRNAs are also efficiently translated.

3.2. *Distribution of nitrate reductase mRNPs*

The distribution of nitrate reductase mRNPs (NR mRNPs) in the polysomes and the post-polysomal supernatant under induced (nitrate as a sole source of nitrogen) and repressed (ammonia as a sole source of nitrogen) conditions was investigated. Under conditions of nitrate induction 85.3% of the NR mRNPs were detected in polysomes while only 14.7% were found as free mRNPs. Upon growth in ammonia, the steady-state levels of nitrate reductase mRNPs were severely inhibited (78%). Of the small amount present, the distribution was 20.8% in the polysomes and the rest as free mRNPs.

3.3. *Polypeptides of mRNP complexes*

The proteins of PmRNPs and FmRNPs eluted at 45°C were extracted and analysed by SDS-PAGE. The PmRNP complexes contained as many as 15–20 polypeptides ranging in molecular weight between 66 and 14 kD. The global population of FmRNPs is associated with only 10–13 polypeptides ranging in molecular weight between 72 and 14 kD. These two classes of mRNPs have common polypeptides as well as an exclusive complement of proteins.

These polypeptides were analysed by two-dimensional gel electrophoresis. The PmRNP proteins were found to be more basic than FmRNPs. The polypeptides also resolved into several isoforms indicating the existence of post-translational modification.

3.4. *Isolation of polyadenylate and CAP-binding proteins*

The cytoplasmic poly(A)$^+$-binding proteins (PABPs) were purified from the polysomes and post-polysomal supernatant[5]. The polypeptides common to both fractions were of 66 and 24 kD. The additional polypeptides associated with the polysomes had molecular weights of 54 and 42 kD. The cap-binding proteins (CBPs) of 15 and 14 kD were purified from the polysomes and post-polysomal supernatant using 7-methyl GTP-sepharose column affinity chromatography[6].

3.5. *In vivo phosphorylation and glycosylation of mRNP proteins*

The FmRNPs in contrast to their PmRNP counterparts were heavily phosphorylated. The prominent FmRNP phosphoproteins included the 52, 47, 42, 38, 27, 23, 22 and 14 kD polypeptides. The 14 kD PmRNP polypeptide was also heavily phosphorylated. On two-dimensional gel electrophoresis several of the FmRNP polypeptides resolved into isoforms. The nature of the phosphoamino acids[7] was phosphoserine and phosphothreonine in FmRNPs and PmRNPs, respectively. The mRNPs were isolated from cells grown in the presence of ^{14}C-glucosamine and analysed by SDS-PAGE. A few low-molecular weight polypeptides were observed in the fluorogram. These polypeptides were however not detected by conA-FITC or periodic acid-Schiff base staining. It therefore appears that glycosylation is not a prominent post-translational modification of mRNP proteins.

3.6. *Enzymatic activities associated with mRNP proteins*

The purified PmRNPs and FmRNPs showed kinase activity in the absence of exogenous substrates. The activity of the FmRNP protein kinase was 4.4 times higher than that of PmRNP kinase. The PmRNP polypeptides were poorly phosphorylated *in vitro* and had molecular weights of 48, 38, 21 and 20 kD. The FmRNP phosphoproteins had molecular weights similar to the *in vivo* phosphoproteins. The nature of the phosphoamino acids was phosphoserine and phosphothreonine. The presence of phosphatase activity was detected in FmRNP preparations. This protein phosphatase has a specific activity of 1.97 mU/mg protein. This protein phosphatase may be capable of reversing the action of protein kinase which is also associated with these complexes. No phosphatase activity could be detected in PmRNP sample.

4. Conclusion

In *C. utilis* there exists two classes of cytoplasmic mRNP complexes. The cytoplasmic localisation of an mRNP species into the polysomes or post-polysomal supernatant determines its translatability. Either the difference in the proteins or the differences in their post-translational modifications (phosphorylation) could determine whether the mRNPs would be integrated into the polysomes and be translated (PmRNP) or be free in the cytoplasm and not be translated (FmRNP). This in turn may be regulated by associated kinase and phosphatase activities.

References

1. WICKERHAM, L. J. — *J. Bact.*, 1946, **52**, 293.
2. JAIN, S. K., PLUSKAL, M. G. AND SARKAR, S — *FEBS Lett.*, 1979, **97**, 84.
3. HENSHAW, E. C. — In *Methods in Enzymology*, Vol. 59 (Colowick, S. P. and Kaplan, N. D., eds), p. 410, 1979, Academic Press.
4. JEFFERY, W. R. — *J. Biol. Chem*, 1977, **252**, 3525.
5. SAMBROOK, J., FRITSCH, E. F. AND MANIATIS, T. — In *Molecular cloning—a laboratory manual*, Second edn, 1989, Cold Spring Harbour Press, USA.
6. WEBB, N. R., CHARI, R. V. J., DE PILLUS, G., KOZARICH, J. W. AND RHOADS, R. E. — *Biochemistry*, 1984, **23**, 177.
7. HUNTER, T. AND SHEFTON, B. M. — *Proc Natn Acad. Sci. USA*, 1980, **77**, 1311.

Thesis Abstract (Ph. D.)

Crystal structure of peanut lectin at 2.95 Å resolution by Rahul Banerjee

Research supervisor: M. Vijayan

Department: Molecular Biophysics Unit

1. Introduction

Lectins are carbohydrate-binding proteins of nonimmune origin. In recent years there has been a spurt in lectin research on account of their ability to specifically bind to cell surface carbohydrates and in view of their diverse applications. The seeds of leguminous plants are a rich source of lectins. Peanut lectin, a legume lectin which is the subject matter of the present investigation exhibits specificity for the T-antigen (Galβ3GalNAc). At physiological pH, it exists as a tetramer with molecular weight 110,000 and four identical polypeptide chains. The earlier work on lectin in this laboratory has been concerned with crystallization, characterization of the crystals and attempts at structure solution using the molecular replacement method[1–4].

2. Experimental

An orthorhombic crystal form (space group $P2_12_12$, $a = 129.3$, $b = 126.9$ and $c = 76.9$ Å) was used in the unsuccessful molecular replacement studies and also in the subsequent work reported here using the multiple isomorphous replacement (MIR) method. In all, six heavy atom derivatives were prepared. An iodine derivative was prepared by replacing lactose with iodophenylgalactose in crystallization experiments, while three platinum derivatives, a samarium derivative and a gold derivative were prepared by controlled soaking. Diffraction data from the native and the derivative crystals were collected on a Siemens–Nicolet area detector mounted on a GX-20 Marconi Avionics rotating anode X-ray generator. One crystal was used for collecting each data set and the raw data were processed using XENGEN. The heavy atom positions were determined using difference Patterson and Fourier maps and the direct methods program MULTAN. Refinement of heavy atom parameters and phase angle calculations were carried out using PHARE in the CCP4 program package (Daresbury Laboratory, England).

The final MIR phase angle calculations yielded a mean figure of merit of 0.49 for 17068 reflections up to a resolution of 3.3 Å. Despite the comparatively low figure of merit, a substantial part of the resulting map was interpretable in terms of features expected in view of homology with concanavalin A (ConA)[5]. Detailed search revealed the presence of a molecular dyad on which the map was averaged. Approximately 82% of the atoms in the tetramer, encompassing almost all the sheets and parts of the loops, could be fitted into the averaged map using FRODO on an IRIS-4D workstation. Subsequently another round of fitting was performed on the unaveraged MIR map. Several cycles of refinement using Hendrickson–Konnert restrained least squares method and model building using electron-density maps calculated with $2F_o–F_c$ as coefficients, and the gradual introduction of higher resolution data resulted in the current model which contains 6919 protein atoms accounting for 97% of a total of 7120 nonhydrogen atoms in the molecule. Five C-terminal residues in all the four subunits and a few side chain atoms could not be located. Solvent atoms have not been included in the refinement. The current R value is 0.218 for 22155 reflections in the 10–2.95 Å resolution shell. The root mean square deviation from the ideal values in bond lengths is 0.025 Å.

3. Results and discussion

Each subunit has essentially the same characteristic tertiary fold found in other legume lectins. The structure, however, exhibits a novel quaternary arrangement of subunits. Contrary to expec-

tations[6] and unlike other well-characterised tetrameric proteins with identical subunits, peanut lectin has neither 222 (D_2) symmetry nor fourfold (C_4) symmetry[7]. A noncrystallographic twofold axis relates to two halves of the molecule. The two monomers in each half are related by a local twofold axis. The mutual disposition of the axes is such that they do not lead to a closed point group. Furthermore, the structure of peanut lectin demonstrates that differences in subunit arrangement in legume lectins could be due to factors intrinsic to the protein molecule and, contrary to earlier suggestions[8,9], are not necessarily caused by interactions involving covalently linked sugars. The framework provided by the structure has been used to explore the structural basis of the variability in the subunit arrangement of legume lectins despite all of them having the same subunit structure. It has also been used to discuss the general problem of 'open' quaternary assembly in proteins.

4. Appendices

While pursuing structural studies on peanut lectin, the author has been involved in the preparation and the characterization of four crystal forms of the lectin from jackfruit (*Artocarpus integrifolia*)[10]. This work, which led to a revaluation of the molecular weight of the protein, is described in an appendix. Another appendix deals with the derivation of relationships among the subunits in peanut lectin. A third appendix is concerned with the crystal structure of iodophenylgalactose which was used for preparing a heavy atom derivative of peanut lectin crystals.

References

1. SALUNKE, D. M., KHAN, M. I., SUROLIA, A. AND VIJAYAN, M. — *J Mol Biol.*, 1982, **154**, 177–178.
2. SALUNKE, D. M., KHAN, M. I., SUROLIA, A. AND VIJAYAN, M. — *FEBS Lett*, 1983, **156**, 127–129.
3. SALUNKE, D. M., SWAMY, M. J., KHAN, M. I., MANDE, S. C., SUROLIA, A. AND VIJAYAN, M. — *J Biol Chem.*, 1985, **260**, 13576–13579.
4. MANDE, S. C. *et al.* — *Indian J Biochem Biophys*, 1988, **25**, 166–171.
5. BECKER, J. W., REEKE, G. N., WANG, J. L., CUNNINGHAM, B A AND EDELMAN, G. M. — *J Biol Chem*, 1975, **250**, 1513–1524.
6. MONOD, J., WYMAN, J. AND CHANGEUX, J.-P. — *J Mol. Biol*, 1965, **12**, 88–118.
7. BANERJEE, R *et al.* — *Proc. Natn. Acad Sci. USA*, 1994, **91**, 227–231.
8. SHAANAN, B., LIS, H. AND SHARON, N. — *Science*, 1991, **254**, 862–865.
9. DELBAERE, L. T. J. *et al.* — *Can. J. Chem.*, 1990, **68**, 1116–1121
10. BANERJEE, R., DHANARAJ, V., MAHANTA, S. K., SUROLIA, A. AND VIJAYAN, M. — *J Mol. Biol*, 1991, **221**, 773–776.

Thesis Abstract (Ph. D.)

Studies on the degradative behaviour of polymers containing weak links of group VIA elements by K. Ganesh

Research supervisor: K. Kishore

Department: Inorganic and Physical Chemistry

1. Introduction

Unavoidable interaction of aerial oxygen during the commercial synthesis of vinyl polymers leads to the insertion of weak–peroxy linkages into the backbone[1, 2] which drastically influence the stability of the polymers even though the peroxy content in the chain may be very small. Although extensive investigations have been carried out on the mode of insertion of peroxy linkages in the polymers[1, 3], unfortunately, our understanding of the effect of weak links on the thermal and photostability of polymers is very poor[4, 5]. Besides the peroxy links, other weak links of group VIA elements, namely, the disulfide and the diselenide linkages also affect the thermal stability of the polymers[6–8].

The main theme of the present investigation is to carry out a comparative study on how the weak links of group VIA elements influence the thermal degradation behaviour of polymers. While most of the data on the copolymers of styrene and oxygen have been taken from the earlier studies of this laboratory[9–11], in the present study, we have synthesized other corresponding new copolymers of group VIA elements, namely, poly(styrene disulfide), PSD; poly(styrene tetrasulfide), PST, and poly(styrene diselenide), PSDSE, for the purpose of comparison with the polymers of group VIA family. The ditelluride polymer of the group, *i.e.*, poly(styrene ditelluride), could not be synthesized due to the high instability of C–Te and Te–Te bonds.

Pyrolysis has been carried out mainly by direct pyrolysis–mass spectrometry (DP-MS) and pyrolysis–gas chromatographic (Py-GC) techniques. The advantage of DP-MS technique is that the primary pyrolysis products here are exclusively detected which is important in studying the primary degradation mechanism of polymers. In addition to DP–MS analysis, the Py–GC–MS studies which give information on final degradation products, have also been carried out on PSD and PST. Hence, the DP–MS and Py–GC techniques are essential to get a complete picture of the pyrolytic behaviour of polymers

2. Results

2.1. *Syntheses and characterization of polymers*

The following new polymers were synthesized and characterized by ^{1}H NMR, ^{13}C NMR, IR, UV spectroscopy and elemental analysis[12].

2.2. *Microstructural details*

From the MS studies, it was found that PSD basically contains a disulfide backbone along with monosulfide linkages to some extent. The PST contains mono-, di- and trisulfide linkages in addition to the major tetrasulfide linkages[13].

PSD 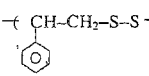

PST 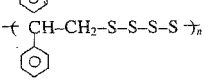

PSDSE 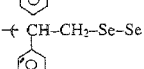

Table I
Summary of pyrolysis data

Technique	*PSP*	*PSD*	*PST*	*PSDSE*
DP–MS	Benzaldehyde, Formaldehyde	Styrene, sulfur cyclic sulfides having the structure (St-S_2) (St = styrene unit) (x = 1–4) and (St$_2$-S_x) (x = 2–4)	Styrene, sulfur, cyclic sulfides having the structure (St-S_x) (St = styrene unit) (x = 1–6) and (St$_2$-S_x) (x = 2–8)	Styrene, selenium
Py–GC (400°C)	Benzaldehyde Formaldehyde	Styrene, sulfur, thiols, CS_2, etc.	Styrene, sulfur and diphenyl thiophene	
Py–GC (610°C)		Styrene, sulfur and negligible amounts of thio and organic compounds	Styrene, sulfur and negligible amounts of thio and organic compounds	

2.3. *Degradation studies*

The degradation of various polymers is summarized in Table I.

The DP–MS analysis reveals an interesting trend down the group with respect to monomer formation. In PSP neither styrene is formed nor oxygen is evolved whereas in PSDSE only the monomers, styrene and selenium metal are obtained. PSD and PST show a mixed products spectrum which contains cyclic sulfides in addition to the monomers, styrene and sulfur[13].

The degradation of PSP is very different from the other candidates of the group in that it exhibits unusual exothermic degradation[14]. This unique behaviour of PSP is attributed to the nature of the degradation products wherein monomers are completely absent. The diverse nature of the degradation products of these group VIA polymers also emanates from the reactivities of alkoxy and thiyl radicals which differ significantly. Under Py–GC conditions at 400°C, the PSD products can be explained by the cleavage of C–S, S–S and C–C bonds. But in PST the C–C cleavage does not occur. Styrene dimer formation which occurs in PSD is absent in PST. Regarding the formation of styrene and sulfur from PSD and PST using DP–MS and Py–GC (400°C and 610°C) analysis, it was found that both the pyrolyzates (styrene and sulfur) are formed in large concentrations when the temperature of pyrolysis is very high (610°C). This is explained by the decrease in radical recombination and rearrangement reactions at high temperatures.

2.4. *Chemical degradation*

The reactivity of S–S linkages of PSD and PST with triphenylphosphine, TPP, has been studied. PSD does not react with TPP at room temperature unlike PST which reacts spontaneously. DP–MS technique was used to analyze the degradation products. Ionic mechanism has been proposed which involves the formation of phosphonium salt followed by the mercaptide–S–S interchange reaction[15].

References

1. BHANU, V. A. AND KISHORE, K. *Chem Rev.*, 1991, **91**, 99–117.
2. GEORGE, G. A AND HODGEMAN, D. K. *Eur Polym J.*, 1977, **13**, 63–71.
3. MOGILEVICH, M. M. *Russ. Chem. Rev*, 1979, **48**, 199–211.
4. MINSKER, K. S. *et al.* *J Macromol. Sci. Rev. Macromol. Chem. C*, 1981, **20**, 243–308 and references cited therein.

5.	WEIR, N. A. AND MILKIE, T. H.	*Makromol Chem.*, 1978, **179**, 1989–1998.
6.	BRUNO, G. *et al.*	*Polymer*, 1977, **18**, 1149–1151.
7.	GHAFOOR, A. AND STILL, H. R.	*J Appl Polym Sci.*, 1977, **21**, 2905–2912.
8.	TANAKA, S. *et al.*	*Makromol Chem Rapid Commun.*, 1983, **4**, 231–235.
9.	KISHORE, K. AND RAVINDRAN, K.	*J Anal Appl. Pyrol.*, 1983, **5**, 363–370.
10.	KISHORE, K. AND RAVINDRAN, K.	*Macromolecules*, 1982, **15**, 1638–1639
11.	KISHORE, K.	*J Therm Anal*, 1981, **21**, 15–19.
12.	KISHORE, K. AND GANESH, K.	*Macromolecules*, 1993, **26**, 4700–4705.
13.	MONTAUDO, G. *et al.*	*J. Anal Appl. Pyrol.*, 1994, **29**, 207–217.
14.	KISHORE, K. AND MUKUNDAN, T.	*Nature*, 1986, **324**, 130–131.
15.	GANESH, K. AND KISHORE, K.	*Polymer science '94–Recent advances* (I. S. Bharadwaj, ed.), 1994, pp. 888–893. Allied Publishers

Thesis Abstract (Ph. D.)

Studies on the miscibility of poly[aromatic (meth)acrylate]s with styrene based polymers by M. Sankarapandian

Research supervisor: K. Kishore

Department: Inorganic and Physical Chemistry

1. Introduction

In spite of rapid developments in polymer syntheses, there are only a handful of polymers which are used in bulk for technological applications. Blending of polymers offers a convenient and economic means of producing materials with varied properties[1,2] and hence the concept of blending is drawing considerable current interest. Blending is also attractive in that diverse polymers, independent of the method of synthesis, can be mixed. The importance of blending can be gauged from the rapid academic and applied progress that has been achieved in the last two decades. In spite of this, the molecular level understanding of polymer miscibility in its various subtle facets is still lacking. The miscibility in polymer blends is greatly negated due to the adverse entropy of mixing[3] and hence it can be promoted only through exothermic mixing. Thus, the

Table I

	Approach	*Systems investigated*
1	Copolymer effect	Acrylonitrile-styrene(AS) copolymers/poly(phenyl acrylate), poly (benzyl-(meth)acrylate)s blends PS/benzyl methacrylate–acrylonitrile (BAN) copolymer blends. AS copolymer/BAN copolymer blends AS copolymer/benzyl methacrylate–styrene(BS) copolymer blends BAN copolymer/BS copolymer blends
2.	Ionic interactions	Benzyl methacrylate-4-vinyl pyridine copolymer/sulfonated polystyrene blends
3.	Hydrogen bonding	Poly(benzyl methacrylate)/styrene-4-hydroxy styrene copolymer blends
4.	Charge transfer interactions	Poly(3,5-dinitro benzoyloxy ethyl methacrylate)/poly(4-N, N-dimethyl amino styrene) blends

preparation of homogeneous polymer blends is one of the challenging areas in polymer science. At an academic level, the problem of understanding the phase behaviour of the polymer blends, in terms of the chemical structures of the polymers, is of paramount importance.

Polymers can be made miscible by promoting exothermic mixing through copolymer effect[4,5] or through specific interactions like hydrogen bonding[6], ionic interaction[7], charge transfer interaction[8], etc. Currently more attention is being paid in the literature to the so-called copolymer effect [9,10]. The copolymer-induced miscibility is called copolymer effect where the miscibility emanates from the mutual repulsion between the comonomer pairs of the copolymer. Recently, it has been demonstrated that in blends consisting of copolymers as one or both the components, miscibility is observed over a range of copolymer compositions, even in the absence of any specific interactions. Although there are several studies in literature on promoting miscibility through copolymer effect[11] and specific interactions, we do not have a clear comparative view on the relative advantages of these approaches. It was therefore thought appropriate to carry out studies on the comparative merits of these methods to get a comprehensive picture and this forms the main objective of the present investigation.

Depending upon the nature and the extent of interactions, the level of segmental miscibility varies significantly in polymer blends. Various techniques are employed to detect the level of miscibility which vary significantly in themselves. For example, optical clarity and differential scanning calorimetry (DSC) are not capable of detecting microheterogeneities lower than 1000 Å and 150 Å, respectively, compared to nonradiative energy transfer (NRET) and solid-state NMR techniques which can probe the miscibility in the range of 30 Å. The study of the level of mixing by different techniques like DSC, NRET and solid-state NMR, forms another objective of the present investigation.

Immiscible systems of poly(aromatic (meth) acrylate)s/polystyrene (PS) blends have been chosen and appropriate modifications were carried out to make the blends miscible under different mechanistic approaches (Table I).

The miscibility behaviour in poly(vinyl chloride) (PVC)/poly(phenyl methacrylate) blends has also been studied.

2. Results and discussion

2.1. *Copolymer effect*

Miscibility in poly(aromatic (meth)acrylate)s/PS blends has been attempted through copolymer effect mechanism by incorporating acrylonitrile units in PS chains. Thus, the polyacrylates and methacrylates were blended with different AS copolymers. AS copolymers have been chosen in this study, as it has been demonstrated in the literature that there exists a strong mutual repulsion

Table II

System	*Miscibility window limits (AN wt% in AS copolymers)*	*Interaction energy density (B_g) values (cal cm^{-3})*	
PPA*/AS copolymers	14.6–34.1	BPA-AN = 3.98;	BPA-St =0.28
PPMA*/AS copolymers	9.5–34.1	BPMA-AN = 4.00;	BPMA-St = 0.20
PBMA*/AS copolymers	7.8–24.3	BBMA-AN = 4.80;	BBMA-St = 0.11
PBA*/AS copolymer	No miscibility window		

*PPA = Poly(phenyl acrylate); PPMA = Poly(phenyl methacrylate); PBMA = Poly(benzyl methacrylate; PBA = Poly(benzyl acrylate).

between the acrylonitrile and styrene units in the copolymers. Miscibility window limits have been identified for these systems from glass transition temperature (T_g) measurements and from these limits the binary interaction energy density parameters (B_{ij}s) were calculated. Using these values, miscibility in other homopolymer–copolymer and copolymer–copolymer systems has been predicted and verified experimentally.

The miscibility window limits and the B_{ij} values calculated in poly(aromatic (meth)acrylate)s/AS copolymer blends are shown in Table II.

It may be pointed out that PBA does not exhibit a miscibility window with AS copolymers. This has been explained from the possible intramolecular hydrogen bonding in PBA. The miscibility window in PBMA/AS copolymer system, as observed by DSC, shows a considerable narrowing in NRET measurements as this technique is more sensitive[12].

2.2. *Ionic interactions*

Ionic interactions were brought about by introducing sulfonic acid groups in PS and basic 4-vinyl pyridine groups in PBMA chains. Ionic interactions result during the acid–base neutralization of the blends. These interactions were confirmed by FTIR studies. As the ionic interactions are stronger, very small concentrations (about 4 mol%) of the interacting groups are sufficient to induce miscibility. By increasing the number of interacting sites, a highly crosslinked network results. At lower concentrations, gelation occurs which was confirmed by viscometry.

2.3. *Hydrogen bonding and charge transfer interactions*

Hydrogen bonding in these blends was achieved by introducing phenolic groups in PS chains. Since hydrogen bonding acceptor ester groups are already present in the methacrylate component, the modification on only one component, namely, PS is sufficient to achieve miscibility. Modification of approximately 5 mol% of PS by phenolic groups is sufficient to induce miscibility. Interestingly the complete modification of PS with phenolic groups results in partially miscible blends due to intramolecular hydrogen bonding.

In order to introduce charge transfer interactions, electron donor groups of N, N-dimethyl amino groups in PS and electron acceptor groups of 3, 5-dinitro benzoyl groups in methacrylates were incorporated. However, the charge transfer interaction was not strong enough to induce miscibility in these systems.

2.4. *Comparison of the various modes of interactions*

Miscibility in poly(aromatic (meth)acrylate)s/PS blends can be achieved through copolymer effect when a minimum of 14 mol% of acrylonitrile units are incorporated in PS. Though an ionic interaction requires only 4 mol% of interacting sites in both the components to induce miscibility, it needs the structures of both the components to be modified. Also, at higher concentrations of the interacting sites, insoluble crosslinked gels were obtained. When 5 mol% of hydrogen bond donor groups of phenolic units are incorporated in PS, miscibility is observed. Comparison of the above results suggests that hydrogen bonding mechanism is the most convenient way to induce miscibility.

2.5. *PVC/PPMA blends*

Poly(vinyl chloride) (PVC)/poly(alkyl (meth)acrylate)s blends are industrially important. Though the phase behaviour of several poly(alkyl methacrylate)s/PVC blends have been reported, studies

on poly(aromatic methacrylate)s/PVC blends are scarce. This system has an advantage in that the phase behaviour can be easily controlled by introducing functional groups in the phenyl rings The phase behaviour of PPMA/PVC blends has been studied in the present investigation. From T_g measurements, this system is found to be miscible, suggesting that the level of miscibility is less than 150 Å. The miscibility in this system is due to weak hydrogen bonding as is evident from FTIR studies. The solid-state NMR rotating frame proton relaxation time Tlrho(H) studies indicate that this system exhibits heterogeneity at 30 Å level.

References

1. OLABISI, O., ROBESON, L. M. AND SHAW, M. T. — *Polymer–polymer miscibility*, 1979, Academic Press.
2. PAUL, D. R. AND NEWMAN, S (EDS) — *Polymer blends*, Vols I & II, 1978, Academic Press
3. FLORY, P. J. — *Principles of polymer chemistry*, 1953, Cornell University Press.
4. PAUL, D. R. AND BARLOW, J. W — Polymer, 1984, 25, 487.
5. ROE, R. J. AND RIGBY, D. — *Adv Polym. Sci*., 1987, **82**, 103.
6. PAINTER, P. C., PARK, Y. AND COLEMAN, M. M. — *Macromolecules*, 1989, **22**, 570.
7. NATANSHON, A., MURALI, R. AND EISENBERG, A. — *Makromol. Chem. Macromol Symp.*, 1988, **16**, 175.
8. RODRIGUEZ, J. M. AND PERCEC, V. — *Macromolecules*, 1986, **19**, 55.
9. NISHIMATO, M , KESKKULA, H. AND PAUL, D. R. — *Macromolecules*, 1990, **23**, 3633.
10. SANKARAPANDIAN, M. AND KISHORE, K. — *Macromolecules*, 1991, **24**, 3090.
11. WALSH, D. J. — *Comprehensive polymer science, polymer properties*, (Booth, C. and Price, C., eds), Vol. 2, p. 135, 1989, Pergamon Press
12. MORAWETZ, H. — *Science*, 1988, **240**, 172.

Thesis Abstract (Ph. D.)

Theoretical studies on models for organic ferromagnetism by Bhabadyuti Sinha

Research supervisor: S. Ramasesha

Department: Solid State and Structural Chemistry Unit

1. Introduction

The thesis examines the three models in existence which predict ferromagnetism in purely organic systems. These models are (i) Mataga–Ovchinnikov[1,2] model which predicts high-spin ground state in alternant polymers with degenerate, nondisjoint, nonbonded molecular orbitals, (ii) McConnell's mechanism I[3] which predicts a high-spin ground state when two radicals are so stacked as to have registry between sites with positive spin density site on one molecule and negative spin density site on another molecule, and (iii) McConnell's mechanism II[4] which predicts a high-spin ground state in a donor–acceptor stack if the lowest virtually excited state is a

high-spin state. In this thesis, with the help of interacting many-body model Hamiltonians, we study the stability of the high-spin states in the parameter space of the models as well as with respect to various perturbations. The models employed are one- and multiband Hubbard and Pariser–Parr–Pople (PPP) models and spin–1/2 Heisenberg model.

2. Results and discussion

We briefly review the electronic properties of organic solids with particular emphasis on magnetism. Several models for organic ferromagnetism are introduced and the current experimental and theoretical status is presented. We then introduce model Hamiltonians necessary for a quantitative study of π-conjugated organic systems, in the context of magnetism. The VB technique for solving these model Hamiltonians is briefly discussed.

The stability of the high-spin ground state in a typical Mataga[1] polymer with respect to breaking the alternancy symmetry and distortion of the backbone conjugation has been examined[5]. In the PPP and Hubbard models the ground state continues to be a high-spin state, even when alternancy symmetry is broken by introducing large site energy differences. The bond order calculations in all these models show that the low-spin state is susceptible to dimerization of the backbone. In the distorted chains, the low-spin state is stabilized to a greater extent leading to low-spin ground states at least in 'soft' lattices.

McConnell's second mechanism[4] based on intramolecular exchange is examined. We find that radicals and radical ions of cyclic polyenes do not give a stable high-spin state. This is attributed to weak intramolecular Hund's rule exchange. However, intra-atomic Hund's rule exchange is much stronger and hence we examine the stacked acetylenic ion–radical systems. The acetylenic ion–radical system is found to possess a high-spin ground state which is stable with respect to different geometries of packing and substitutions[6]. The stability of the high-spin state is attributed to the degeneracy of the atomic orbitals involved in conjugation. These systems are suggested to be prime candidates for observing organic ferromagnetism.

We examine in detail the competition between kinetic exchange and direct exchange in McConnell's second mechanism[4] for organic ferromagnetism. We employ multiband Hubbard and PPP models to study mixed donor–acceptor stacks with doubly degenerate acceptor orbitals and nondegenerate donor orbitals at 2/3rd filling[7]. Model exact results for 2, 3 and 4 D-A units show that McConnell's prediction of high-spin ground state in these systems[4] is in general incorrect. The larger phase–space available for low-spin state leads to its kinetic stabilization in preference to high-spin states. However, for large electron correlation strengths, the direct exchange dominates over the kinetic exchange resulting in a high-spin ground state.

We study the McConnell's spin density model[3] for organic ferromagnetism. Typically, molecules which belong to this class are pseudo- ortho-, meta- and para-dicarbene-substituted [2, 2] paracyclophanes. We employ a Heisenberg spin model in these studies as the number of active orbitals is too large to include charge degrees of freedom in an exact calculation. The ground state is always a quintet in psuedo-ortho and para isomers and the lowest energy spin excitation is to a triplet state while the pseudo-meta isomer possesses a singlet ground state[8]. The possibility of obtaining high-spin molecules and eventually an organic ferromagnet in one dimension as was proposed by McConnell[3] seems justified.

3. Conclusions

The regular Mataga polymers exhibit stable high-spin state. In the distorted chains, the low-spin state is stabilized to a greater extent leading to low-spin ground states at least in 'soft' lattices.

Radicals and radical ions of cyclic polyenes do not give a high-spin state. The acetylenic ion-radical system is found to possess a high-spin ground state which is stable with respect to different geometries of packing and substitutions. In D-A polymers, for large correlation strengths, the direct exchange dominates over kinetic exchange resulting in a high-spin ground state. The ground state is always a quintet in pseudo-ortho and para paracyclophanes and the lowest energy spin excitation is to a triplet state while the pseudo-meta isomer possesses a singlet ground state.

References

1. MATAGA, N. *Theor. Chim. Acta*, 1968, **10**, 372–376.
2. OVCHINNIKOV, A. A. *Theor. Chim. Acta*, 1978, **47**, 297–304.
3. MCCONNELL, H. M. *J. Chem. Phys.*, 1963, **39**, 1910.
4. MCCONNELL, H. M. *Proc. Robert A. Welch Foundation Conf. on Chemical Research*, 1967, Vol. 11, p. 144.
5. SINHA, B., ALBERT, I. D. L. AND RAMASESHA, S. *Phys. Rev. B*, 1990, **42**, 9088–9097.
6. RAMASESHA, S. AND SINHA, B. *Chem. Phys. Lett*, 1991, **179**, 379–384.
7. SINHA, B. AND RAMASESHA, S. *Phys. Rev. B*, 1993, **48**, 16410–16416.
8. SINHA, B. AND RAMASESHA, S. *Chem. Phys Lett.*, 1991, **182**, 180–186.

Thesis Abstract (Ph. D.)

Development of new synthetic methods for organic synthesis by Jagattaran Das

Research supervisor: S. Chandrasekaran

Department: Organic Chemistry

1. Introduction

Oxidations and reductions are two fundamental reactions in organic chemistry. Oxidation of olefins by potassium permanganate has been known for over a century[1]. Since permanganate is highly soluble in aqueous medium, its application has become limited to those substrates which have appreciable solubility in aqueous medium. To overcome this solubility problem, heterogeneous permanganate oxidation with solid supports has become quite popular in the last few years. The oxidising ability of permanganate has been found to be enhanced with solid support $CuSO_4.5H_2O$ in the presence of catalytic amount of water and *tert*-butyl alcohol. A nonclassical phase transfer catalyst, *i.e.*, omega phase[2] has been invoked to explain the role of water and *tert*-butyl alcohol. Oxidations of various olefins and γ-hydroxy olefins have been studied.

Hydration of olefins can be achieved *via* trialkylboranes followed by oxidation with H_2O_2 and NaOH. Conversion of olefins to alcohols with a new reagent system consisting of benzyltriethylammonium borohydride and chlorotrimethylsilane (1:1) in CH_2Cl_2 without any oxidative work-up can also be achieved. A thorough mechanistic study of this unusual hydration of olefins has been undertaken. The same reagent system also converts carboxylic acids to their corresponding alcohols in high yields.

2. Results and discussion

The oxidation of olefins in aqueous medium produces different products depending upon the pH of the medium. During this investigation it has been found that cyclic olefins produce α–

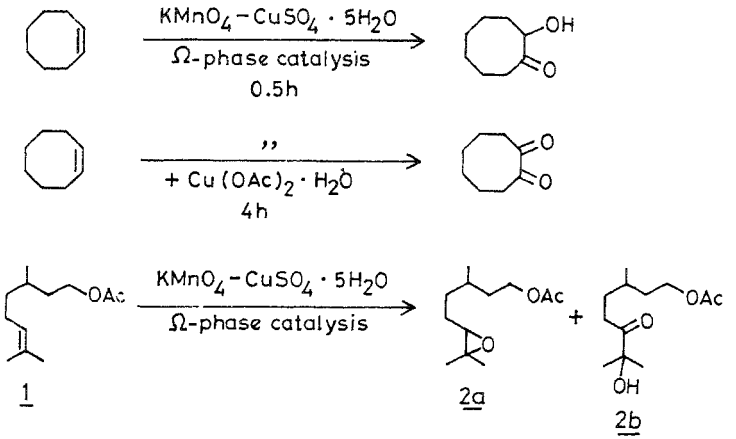

SCHEME 1.

ketols/α-diketones with $KMnO_4$–$CuSO_4 \cdot 5H_2O$ under omega phase catalysis. Citronellol acetate **1** produces appreciable amount of epoxide **2a** apart form α-ketol **2b** (Scheme 1)[3].

The conditions for the formation of epoxide observed earlier have been optimized. It is found that lipophilic substrates have a tendency to form epoxide under the reaction conditions and maximum amounts can be the obtained when $KMnO_4$–$CuSO_4 \cdot 5H_2O$ has been used as oxidant under omega phase catalysis using dichloromethane as solvent. The epoxide formation can be reduced or eliminated if montmorillonite K-10 is used as a solid support instead of $CuSO_4 \cdot 5H_2O$ under identical conditions. The methodology can be used for the oxidation of oleic acid derivatives to the corresponding α-diketones.

Studies related to the reaction of Δ^5-unsaturated steroids with heterogeneous permanganate under omega phase catalysis have also been described. Interestingly, it has been found that in all the steroids studied 5β, 6β-epoxide is formed with high degree of stereoselectivity (>92%) in very good yield (90–95%) (Scheme 2).

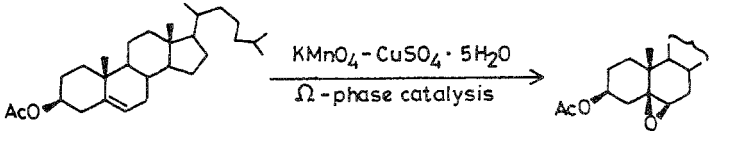

SCHEME 2.

While numerous methodologies for the cyclopentenone annulation are available, one that generates 5, 5-dimethylcyclopentenone directly from carbonyl precursors is not that common. Studies related to the development of such a methodology using substituent-directed oxidative cyclisation has been described. Similarly, allylic spiro-lactones 3 which have earlier been prepared by a circuitous route have been synthesised easily in good yield using this methodology. A short synthesis of steroidal spiro-lactone has also been achieved (Scheme 3).

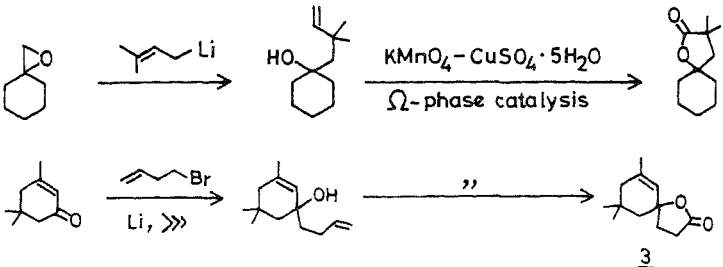

SCHEME 3.

The substituent-directed oxidative cyclisation strategy has been extended to the synthesis of medium-sized cyclic keto-lactones using $KMnO_4$-$CuSO_4$ $5H_2O$ or $KMnO_4$-montmorillonite K-10 under conditions of omega phase catalysis[5] (Scheme 4).

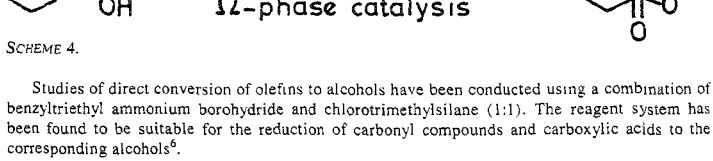

SCHEME 4.

Studies of direct conversion of olefins to alcohols have been conducted using a combination of benzyltriethyl ammonium borohydride and chlorotrimethylsilane (1:1). The reagent system has been found to be suitable for the reduction of carbonyl compounds and carboxylic acids to the corresponding alcohols[6].

Attempts have also been made to delineate the mechanism of the unusual hydration of olefins to alcohols under these conditions. The role of silicon and the incorporation of atmospheric oxygen have been suggested to be responsible for the above transformation.

References

1. FATIADI, A. J. *Synthesis*, 1987, 85.

2. LIOTTA, C. L., BURGESS, E. M., RAY, C. C., BLACK, E. D. AND FAIR, B. E. *ACS Symp. Ser.*, 1987, 326, *Prep. Am Chem. Soc., Div. Pet. Chem.*, 1985, **30**, 367.

3.	BASKARAN, S., DAS, J. AND CHANDRASEKARAN, S.	*J. Org Chem*, 1989, **54**, 5182.
4.	SYAMALA, M. S., DAS, J., BASKARAN, S. AND CHANDRASEKARAN, S.	*J Org Chem*, 1992, **57**, 1928.
5	DAS, J. AND CHANDRASEKARAN, S.	*Tetrahedron*, 1995, **51**, 3389
6.	DAS, J. AND CHANDRASEKARAN, S.	*Synth Commun*, 1990, **20**, 907.

Thesis Abstract (Ph. D.)

On the photodimerization of coumarins in the solid state: structure–reactivity correlation by J. Narasimha Moorthy

Research supervisors: K. Venkatesan and N. Guru Row
Department: Organic Chemistry

1. Introduction

The relationship between the crystal lattice and the course of a reaction has been well established from the seminal contributions of Schmidt *et al.*[1] Proximity and local symmetry between the reacting partners are crucial for the occurrence of a facile photodimerization reaction in the solid state. One approach to realize the required criteria in the crystalline state has focussed on the investigations aimed at preorganising the molecules in a predetermined fashion in the crystal lattice, the study being termed *crystal engineering*. The steering groups such as chloro, bromo, acetoxy, methylenedioxy, etc., are a result of remarkable advances made in this direction[1]. However, engineering of the crystals with a packing motif of one's interest is beyond control, since the weak intermolecular interactions which are of paramount importance in controlling the crystal packing still remain to be well understood. One way this problem is overcome is by 'host–guest' complexation[2] The utility of host–guest complexation to direct photodimerization of coumarins selectively has been illustrated and the solid-state reactivity-correlations of a few substituted coumarins are presented.

2. Results and discussion

Cyclodextrins (CDs) are toroidally shaped oligosaccharides comprising 6–8 (α-, β- and γ-) glucose units linked *via* –1, 4 glycosidic bonds. The unique property of CDs is their ability to form inclusion complexes with a variety of organic compounds. They affect the behaviour of guest molecules through microenvironmental effects and by exerting steric control over the motions of the included guests. Remarkable influence of CD complexation on various photochemical reactions has been reported.

Effect of CDs in the regulation of photodimerization of coumarins and several of its derivatives in the solid state was investigated. Based on the stereochemistry of the photodimers isolated, several hypotheses concerning the location and relative orientations of the guest coumarins in the host toruses were made. Depending upon the substituent, substitution pattern and the type of CD employed, complexes whose host:guest stoichiometry are 1:1, 1:2 and 2:2 were identified. In several instances, dimers not available from irradiation of neat solid coumarins or their solutions were obtained upon irradiation of their CD complexes. The stereochemistry of the dimer obtained upon irradiation of the complex of coumarin and β-CD was unambiguously established to be *syn* head-to-head from single-crystal X-ray diffraction studies. The nature of coumarin/β-CD complex was also established to be 2H:2G type by X-ray structure determination at room temperature.

The diols, 1, 1, 6, 6-tetraphenylhexa-2, 4-diyne-1, 6-diol (Da) and 1,6-bis(*o*-chlorophenyl)-1, 6-diphenylhexa-2, 4-diyne-1, 6-diol (Dc), form inclusion compounds with a variety of organic compounds. Coumarins included in the lattices of the diols Da and Dc were found to undergo efficient photodimerization upon irradiation, *e.g.*, irradiation of 1:2 complex of Dc and coumarin furnishes selectively *syn* head-to-head dimer in a quantitative yield. The chiral diol Dc was found to be remarkable in bringing about the packing of guest coumarins that results in mirror symmetric photodimers upon irradiation. The role of chiral diol Dc was examined by crystal structure analysis of 1:2 complex of Dc and coumarin. The potential of the diol Dc relative to the achiral diol Da was attributed to the ability of Dc to exhibit flexibility in packing modes.

During the course of investigation of photodimerization of coumarins when complexed with the inclusion compounds described earlier, 7-methoxy-4-methylcoumarin was observed to undergo unusual photodimerization in the solid state yielding two photodimers (Scheme 1), *viz.*, *syn* H–H and *syn* H–T. While the *syn* H–H dimer was found to be a consequence of topochemical photodimerization, the formation of minor *syn* H-T dimer was inferred to be a result of the reaction occurring at the defect sites generated subsequent to the formation of topochemical *syn* H–H dimer.

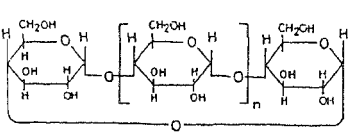

20 (α-CD): n= 4; 21 (β-CD): n= 5; 22 (γ-CD): n= 6

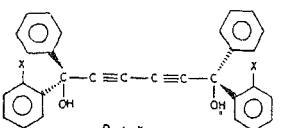

Da: X = H
Dc: X = Cl

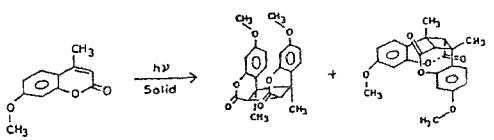

SCHEME 1.

4-Styrylcoumarin, endowed with two reaction sites, was found to crystallize from hexane and chloroform (1:1 mixture) in two crystalline modifications. Upon irradiation, the dimorphs were found to yield regioisomeric *anti* head-to-tail dimers stereoselectively (Scheme 2). The differences in the reactivities of the dimorphs were exemplified from the differences in the packing arrangements of the crystals.

A series of 4, 7-disubstituted coumarins was found to photodimerize in solid state yielding *anti* H–T dimers invariably (Scheme 3), while a different course of reaction path was observed in solution. The photochemical results suggest α-type packing in all the cases. The monochloro substitution was found to be ineffective in these systems. Based on the analyses of the crystal structures of 7-hydroxy-4-styrylcoumarin, 7-methoxy-4-styrylcoumarin and a few cases reported in the literature, C=O...π(aryl) interaction was implied as the driving force for α-packing.

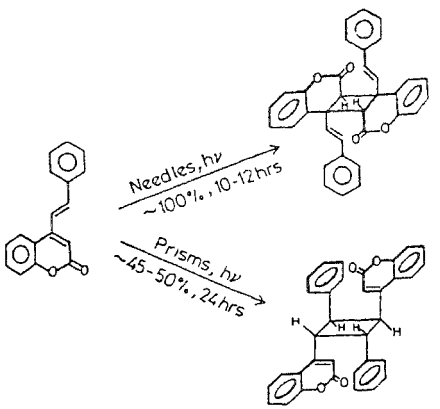

SCHEME 2.

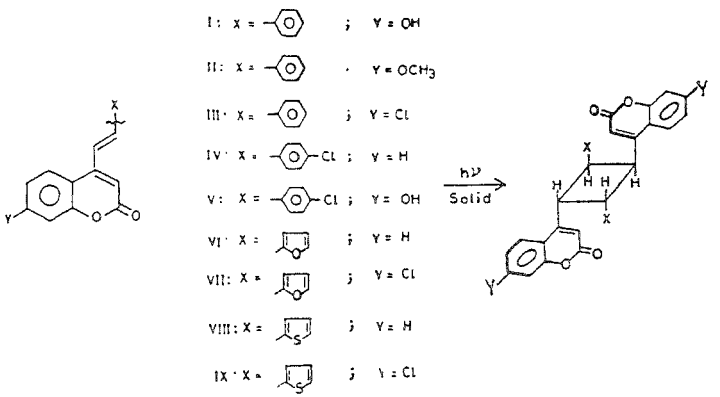

SCHEME 3.

References

1. SCHMIDT, G. M. J. *et al.* — *Solid state photochemistry* (D. Ginsburg, ed), 1976, Verlag Chemie.

2. RAMAMURTHY, V. — *Photochemistry in organized and constrained media*, 1991, VCH Publishers.

Thesis Abstract (Ph. D.)

Theoretical studies of structural and electronic effects in organic reactions by Animesh Pramanik

Research supervisor: J. Chandrasekhar

Department: Organic Chemistry

1. Introduction

This work involves computational investigations on several organic reactions of considerable experimental interest, to obtain detailed insights into the relative importance of various stereoelectronic factors influencing chemical reactivity.

One of the fundamental goals of chemists is to effect chemical transformations in a controlled desired fashion. This requires an intricate knowledge of the course of reactions and the factors influencing them. Theoretical methods are quite powerful to derive valuable information on reaction mechanisms. Several procedures including molecular and semiempirical MO (AM1, MNDO) methods have been used in the present investigation.

2. π-Facial selectivities in cycloaddition reactions

The factors contributing to the experimentally observed π-facial selectivities in the Diels–Alder reaction in two types of substrates have been critically evaluated. The facially perturbed dienophiles, norbornenyl-fused *p*-benzoquinone (NPBQ), **1**, and norbornyl-fused *p*-benzoquinone (DNPBQ), **2**, have been shown to exhibit a range of stereoselectivities in their reaction with various dienes. Molecular mechanics and semiempirical MO calculations as well as a hybrid force field/MO model have been employed to determine the importance of ground-state geometric distortions, orbital interactions, and steric effects in the transition states. Model calculations, exclusively taking into account nonbonded forces between the diene and the dienophile at the transition state, account for the observed product distributions[1].

The observed selectivities in the cycloaddition reactions of a set of facially nonequivalent hexacyclic dienes **3** and **4** have been rationalized. A comprehensive description is provided based on a detailed computational study of the transition state energetics with different types of model dienophiles at the AM1 level. The calculations reveal that the face selectivities of alkynes reflect the intrinsic face selectivity as dictated by the electronic structure of the diene substrate. In the case of alkene-type dienophiles, the steric bias imposed by the cyclobutane ring hydrogen atoms also contribute to face selectivity. The preferred direction of approach of heteroatomic dienophiles like azo derivatives and singlet oxygen is significantly influenced by dipolar repulsions due to the carbonyl oxygen atoms. These interpretations are confirmed through additional calculations carried out with the model diene **5**. Predictions of face selectivities are made for a few more related systems.

3. Theoretical investigation of the factors influencing homo–Diels–Alder reactivity

The [2+2+2] cycloaddition of a 1,4 diene with a dienophile, known as the homo–Diels–Alder reaction, represents a relatively less understood and underexploited procedure. Molecular mechanics calculations have been carried out on a number of experimentally studied nonconjugated dienes[2] to obtain a general appreciation of the geometric and strain energy constraints which need to be satisfied for facile homo–Diels–Alder reactivity. More detailed insights have been obtained from MO calculations of the energy profiles for representative systems. The relative preferences

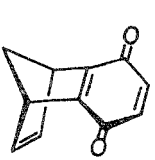

1.

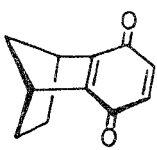

2.

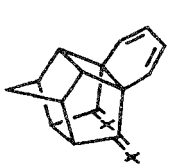

3: $x = 0$
4: $x = CH_2$

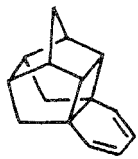

5.

for synchronous and asynchronous transition states have been computed. The calculations reveal a previously unsuspected electronic symmetry factor in the homo–Diels–Alder reaction. Through-bond interactions are shown to be critical in determining the HOMO of the biradicaloid transition state which in turn controls the feasibility of the reaction.

4. Geometric and electronic effects in Bergman and Myers' cyclizations

The importance of orbital symmetry effects in reactions proceeding *via* biradicaloid pathways is demonstrated for another system. AMI calculations with CI have been carried out on a number of substrates potentially capable of undergoing Bergman cyclization. The reaction is currently of great interest in view of its role in the DNA cleaving ability of the enediyne class of antitumor antibiotics, like esperamicin, dynemicin, calichemicin, neocarzinostatin, etc. Simpler models have generally been designed on the basis of geometric and strain criteria[3]. The present semiquantitative MO calculations show the importance of orbital symmetry and through-bond effects in determining the energy profiles of Bergman cyclization reaction. With suitable models, the critical role of these factors is established. The dependence of the activation energies for Myer cyclization in allen-ene-yne systems on the distance between the terminal reacting sites has been computationally evaluated. The results are compared with the known sensitivity of cyclization rates of ene-diyne class of compounds to the distance criterion.

5. Stereo-control of the rates of Claisen rearrangements in unsaturated sugar systems

AMI calculations have been used to rationalize the observed stereo-control of the rates of Claisen rearrangements in unsaturated sugar systems. The relative activation barriers for α- and β-anomeric pairs of vinyl and aryl ethers at different centres of a pyranose ring have been precisely computed. The role of the anomeric effect in determining the ground state conformation and the stability of the transition state as well as steric interactions between the migrating unit and the underlying sugar ring have been analysed with appropriate model systems. The conformational predilictions of the rearranging fragment and the sugar ring have been studied in detail. The computed results are consistent with all available experimental data and have considerable significance for the use of Claisen rearrangements in carbohydrate syntheses.

References

1 MEHTA, G., PADMA, S., PATTABHI, V., PRAMANIK, A. AND CHANDRASEKHAR, J. π-Facial selectivities in cycloadditions to norbornyl- and norbornenyl-fused *p*-benzoquinones, *J. Am. Chem Soc.*, 1990, **112**, 2942–2949.

2. FICKES, G. N. AND METZ, T. E. Scope of the homo–Diels–Alder reaction, *J. Org Chem.*, 1978, **43**, 4057–4061.

3. NICOLAOU, K. C. AND DAI, W.-M. Chemistry and biology of the enediyne anticancer antibiotics, *Angew. Chem Int Ed Engl.*, 1991, **30**, 1387–1416.

Thesis Abstract (Ph. D.)

Physics of Si-related DX center in $Al_xGa_{1-x}As$ and GaAs by Subhasis Ghosh

Research supervisors: Vikram Kumar and Arup Kumar Roy Chowdhury

Department: Physics

1. Introduction

Most of the interesting properties of matter in the solid state are related to the presence of defects and impurities. A localized defect can be created by removing or replacing one crystal atom by an impure atom or by similar operations. There are rather different motivations behind the enormous amount of work in this field. Firstly, defects or impurities, even in small quantities, strongly influence the semiconductor-based device performance, either by creating a certain desired performance or conversely by degrading it. Secondly, it is the theoretical challenge one comes across while attempting to describe the basic physics of defects in solids.

The DX center in III–V semiconductor is a very interesting new class of defects characterized by many fascinating properties which are not commonly observed in other defects in semiconductors. DX center is a donor-related deep level which is found in several ternary alloys when they are doped with group IV (Si,Ge,Sn) or group VI (S,Se,Te) dopants. This deep level is also observed in *n*-type GaAs and InP under hydrostatic pressure. The name 'DX center' was originally proposed by D. V. Lang[1].

The physics of DX centers is certainly very complex and intriguing and there still seems to be room for further improvements in our understanding of this scientifically and technologically important defect. There are many basic doubts and controversies regarding its different properties. One such controversy is related to the effective electron correlation energy U of the DX center. There is even a controversy as to whether the DX center is donor- or acceptor like. There was no idea on the microscopic origin of persistent photoconductivity (PPC). In this work, we have experimentally studied and attempted to explain some of the key issues which will be of immense use in understanding DX centers in $Al_xGA_{1-x}As$ and GaAs.

2. Experimental studies

A new method called photoemission deep-level transient spectroscopy (DLTS) has been used to study Hubbard correlation energy of the DX center. A new spectroscopic technique based on DLTS has been used to determine the capture barrier for the DX center. Transient photoconductivity is used to study the kinetics of photoionization process and microscopic origin of persistent photoconductivity (PPC).

The $Al_xGa_{1-x}As$ ($x = 0.26$, 0.30, 0.33, 0.45) samples used in our study were Si-doped and grown by molecular beam epitaxy (MBE) on semi-insulating substrate. Carrier concentration was determined by Hall and C–V measurements; and AlAs mole fractions were determined by photoluminescence and electron probe microanalysis.

3. Results and discussion

It was predicted[2] by a series of theoretical work that DX center is a negative-U system. The first direct experimental evidence of the negative-U nature of the DX center has been presented by a

new method called photoemission-DLTS[3,4]. According to the negative-U model, DX center should capture two electrons with the second bound more strongly than the first, and the ground state should be negatively charged (DX^-), and the whole system should possess a negative Hubbard correlation energy. In the presence of sub-bandgap light (1.38 eV, 1.21 eV), a new DLTS peak at a low temperature evolves with a thermal activation energy in the range of 200–300 meV in silicon-doped $Al_xGa_{1-x}As$ for different AlAs fractions. It is shown that this photo-induced new level, corresponds to the emission process DX^0, there being two levels in the gap, an acceptor level ($DX^- \rightarrow DX^0 + e^-$), and a donor level ($DX^0 \rightarrow d^+ + e^-$). It is conclusively shown that the acceptor level (–/0) lies below the donor level (0/+). This inverted ordering of the energy levels reveals an effective correlation negative energy with the existence of thermodynamically unstable DX^0 state. The outcome of this experiment also settles a long-standing controversy regarding the charge-state of DX center.

A detailed study of transient growth of the photoconductivity due to DX center in $Al_xGa_{1-x}As$ was performed. Analysis of the photoionization process of the DX center reveals a two-step process which can be fitted with the rate equation using negative-U initial conditions. It has been possible phenomenologically to explain the emission kinetics at different temperatures and different light intensities[5]. This experiment further supports the negative-U nature of the DX center and its acceptor-like nature.

Kinetics of the persistent photoconductivity (PPC) decay has been studied. It was shown for the first time that PPC decay follows the stretched exponential law $n(t) = n(0)\exp[-(t/\tau)^{\beta}]$. It is found that the stretching parameter β and the relaxation time constant τ depends on the temperature with β ranging from 0.2 to 0.4. The stretched exponential relaxation is attributed to the capture-enhanced motion of the silicon–donor atom from substitutional to interstitial site in $Al_xGa_{1-x}As$ lattice during the capture of the photoexcited electrons from the conduction band. Local atomic alloy disorder $Al_xGa_{1-x}As$ causes the distribution of the capture activation energies. The width of these activation energies as determined from the temperature dependence of the stretching parameter β was also verified by the direct measurement of the capture activation energies[6].

DLTS was used to study the deep levels related to DX center in $Al_xGa_{1-x}As$ for different AlAs mole fractions and heavily doped ion-implanted GaAs[7]. By virtue of heavy doping, Fermi level lies within the conduction band and this allows us to observe the capture and the emission of the electrons by the localized DX level resonant with the conduction band using DLTS measurements carried out on a metal-insulator semiconductor (MIS) diode. All the DLTS spectra consisted of multiple peaks, with two dominant ones. The two dominant peaks were deconvoluted, and their emission activation energies were separately measured for different AlAs mole fractions. The existence of two levels due to Si-related DX center in GaAs, rules out alloy broadening as the only cause for multiple levels. It is conjectured that the origin of these two levels may arise due to the splitting of the ground state of DX level through a Coulombic contribution to the intervalley scattering in the L band.

There was large dispersion in the capture activation energy in the literature due to the inherent non-exponentiality in the capture and emission kinetics. The capture activation energy was determined directly by a novel spectroscopic technique[8]. In this technique, we used the fact that the capture time constant is long and strongly temperature dependent due to the large capture barrier. The transient capacitance due to capture was analyzed in the same way as the conventional DLTS by sampling with two gates.

References

1. LANG, D. V., LOGAN, R. A. AND JAROS, M. — *Phys Rev. B*, 1979, **19**, 1015.
2. CHADI, D. J. AND CHANG, K. J. — *Phys Rev. Lett*, 1988, **61**, 873; *Phys. Rev. B*, 1989, **39**, 10063; *Phys Rev. B*, 1993, **47**, 13205.
3. SUBHASIS GHOSH AND VIKRAM KUMAR — *Phys Rev. B*, 1992, **46**, 7533.
4. SUBHASIS GHOSH AND VIKRAM KUMAR — *MRS Symp. Proc. on Defect Engng in Semiconductor Growth, Processing and Device Technology*, 1992, pp. 262, 579.
5. SUBHASIS GHOSH AND VIKRAM KUMAR — *Sol. St Commun.*, 1992, **83**, 37.
6. SUBHASIS GHOSH AND VIKRAM KUMAR — *Europhys. Lett*, 1993, **24**, 779.
7. SUBHASIS GHOSH AND VIKRAM KUMAR — submitted to *J. Appl. Phys.*
8. SUBHASIS GHOSH AND VIKRAM KUMAR — *J Appl. Phys* (in press).